MORPHOLOGY FOR HIGHER-DIMENSIONAL TENSOR DATA VIA LOEWNER ORDERING

Bernhard Burgeth,[1] Nils Papenberg, [1] Andres Bruhn, [1] Martin Welk, [1] Christian Feddern, [1] and Joachim Weickert [1]

[1] *Saarland University*
Faculty of Mathematics and Computer Science
Bld. 27.1, P.O. Box 15 11 50, 66041 Saarbruecken
Germany
{burgeth,papenberg,bruhn,welk,feddern,weickert}@mia.uni-saarland.de

Abstract The operators of greyscale morphology rely on the notions of maximum and minimum which regrettably are not directly available for tensor-valued data since the straightforward component-wise approach fails.
This paper aims at the extension of the maximum and minimum operations to the tensor-valued setting by employing the Loewner ordering for symmetric matrices. This prepares the ground for matrix-valued analogs of the basic morphological operations. The novel definitions of maximal/minimal matrices are rotationally invariant and preserve positive semidefiniteness of matrix fields as they are encountered in DT-MRI data. Furthermore, they depend continuously on the input data which makes them viable for the design of morphological derivatives such as the Beucher gradient or a morphological Laplacian. Experiments on DT-MRI images illustrate the properties and performance of our morphological operators.

Keywords: Mathematical morphology, dilation, erosion, matrix-valued images, diffusion tensor MRI, Loewner ordering

Introduction

A fruitful and extensive development of morphological operators has been started with the path-breaking work of Serra and Matheron [11, 12] almost four decades ago. It is well documented in monographs [8, 13–15] and conference proceedings [7, 16] that morphological techniques have been successfully used to perform shape analysis, edge detection and noise suppression in numerous applications. Nowadays the notion of image also encompasses tensor-valued data, and as in the scalar case one has to detect shapes, edges and eliminate noise. This creates a need for morphological tools for matrix-valued data.

Matrix-valued concepts, that truly take advantage of the interaction of the different matrix-channels have been developed for median filtering [20], for active contour models and mean curvature motion [5], and for nonlinear regularisation methods and related diffusion filters [17, 19]. In [4] the basic operations dilation and erosion as well as opening and closing are transfered to the matrix-valued setting at least for 2×2 matrices. However, the proposed approaches lack the continuous dependence on the input matrices which poses an insurmountable obstacle for the design of morphological derivatives.

The goal of this article is to present an alternative and more general approach to morphological operators for tensor-valued images based on the Loewner ordering. The morphological operations to be defined should work on the set $\mathrm{Sym}(n)$ of symmetric $n \times n$ matrices and have to satisfy conditions such as:

(i) Continuous dependence of the basic morphological operations on the matrices used as input for the aforementioned reasons,

(iii) preservation of the positive semidefiniteness of the matrix field since DT-MRI data sets posses this property,

(iii) rotational invariance.

It is shown in [4] that the requirement of rotational invariance already rules out the straightforward component-wise approach. In this paper we will introduce a novel notion of the minimum/maximum of a finite set of symmetric matrices which will exhibit the above mentioned properties.

The article has the following structure: The subsequent section gives a brief account of the morphological operations we aim to extend to the matrix-valued setting. In section 3 we present the crucial maximum and minimum operations for matrix-valued data based on the Loewner ordering. We report the results of our experiments with various morphological operators applied to real DT-MRI images in section 4. The last section 5 provides concluding remarks .

1. Morphological Operators

Standard morphological operations utilise the so-called *structuring element* to work on images represented by scalar functions $f(x, y)$ with $(x, y) \in I\!R^2$. Greyscale *dilation* $\oplus$, resp., *erosion* $\ominus$ w.r.t. B is defined by

$$\begin{aligned} (f \oplus B)(x,y) &:= \sup\{f(x-x',\, y-y') \mid (x',y') \in B\}, \\ (f \ominus B)(x,y) &:= \inf\{f(x-x',\, y-y') \mid (x',y') \in B\}. \end{aligned}$$

The combination of dilation and erosion gives rise to various other morphological operators such as *opening* and *closing*,

$$f \circ B := (f \ominus B) \oplus B\,, \qquad f \bullet B := (f \oplus B) \ominus B\,,$$

the *white top-hat* and its dual, the *black top-hat*

$$\mathrm{WTH}(f) := f - (f \circ B)\,, \qquad \mathrm{BTH}(f) := (f \bullet B) - f\,,$$

finally, the *self-dual top-hat*, $\mathrm{SDTH}(f) := (f \bullet B) - (f \circ B)$.
The boundaries of objects are the loci of high greyvalue variations in an image which can be detected by gradient operators. The so-called *Beucher gradient*

$$\varrho_B(f) := (f \oplus B) - (f \ominus B)\,,$$

as well as the *internal* and *external gradient*,

$$\varrho_B^-(f) := f - (f \ominus B)\,, \qquad \varrho_B^+(f) := (f \oplus B) - f$$

are analogs to the norm of the gradient $\|\nabla f\|$ if the image f is considered as a differentiable function.

The application of shock filtering to matrix-valued data calls for an equivalent of the Laplace operator $\Delta f = \partial_{xx} f + \partial_{yy} f$ appropriate for this type of data. A *morphological Laplacian* has been introduced in [18]. However, we use a variant given by

$$\Delta_m f := \varrho_B^+(f) - \varrho_B^-(f) = (f \oplus B) - 2 \cdot f + (f \ominus B)\,.$$

This form of a Laplacian acts as the second derivative $\partial_{\eta\eta} f$ where η stands for the direction of the steepest slope. Therefore it allows us to distinguish between influence zones of minima and maxima of the image f, a property essential for the design of shock filters.

The idea underlying *shock filtering* is applying either a dilation or an erosion to an image, depending on whether the pixel is located within the influence zone of a minimum or a maximum [10]:

$$\delta_B(f) := \begin{cases} f \oplus B & \text{if} \quad \mathrm{trace}(\Delta_m f) \le 0\,, \\ f \ominus B & \text{otherwise.} \end{cases}$$

2. Maximal and Minimal Matrices with Respect to Loewner Ordering

In this section we describe how to obtain the suitable maximal (minimal) matrix that majorises (minorises) a given finite set of symmetric matrices. We start with a very brief account of some notions from convex analysis necessary for the following.

A subset C of a vector space V is named *cone*, if it is stable under addition and multiplication with a positive scalar. A subset B of a cone C is called *base* if every $y \in C, y \neq 0$ admits a unique representation as $y = r \cdot x$ with $x \in B$ and $r > 0$. We will only consider a cone with a convex and compact base.

The most important points of a closed convex set are its *extreme points* characterised as follows: A point x is an extreme point of a convex subset $S \subset V$ of a vector space V if and only if $S \setminus \{x\}$ is still convex. The set of all extreme points of S is denoted ext(S). All extreme points are necessarily boundary points, ext(S) $\subset$ bd(S). Each convex compact set S in a space of finite dimension can be reconstructed as the set of all convex combinations of its extreme points [1, 9]: $S = \text{convexhull}(\text{ext}(S))$.

The Cone of the Loewner Ordering

Let Sym(n) denote the vector space of symmetric $n \times n$-matrices with real entries. It is endowed with the scalar product $\langle A, B\rangle := \sqrt{\text{trace}(A^\top B)}$. The corresponding norm is the Frobenius norm for matrices: $\|A\| = \sum_{i,j=1}^{n} a_{ij}$. There is also a natural partial ordering on Sym(n), the so-called *Loewner ordering* defined via the cone of positive semidefinite matrices Sym$^+(n)$ by

$$A, B \in \text{Sym}(n): \quad A \geq B :\Leftrightarrow A - B \in \text{Sym}^+(n),$$

i.e. if and only if $A - B$ is positive semidefinite.
This partial ordering is *not* a lattice ordering, that is to say, the notion of a unique supremum and infimum with respect to this ordering does not exist [3]. The (topological) interior of Sym$^+(n)$ is the cone of positive definite matrices, while its boundary consists of all matrices in Sym(n) with a rank strictly smaller than n. It is easy to see that, for example, the set $\{M \in \text{Sym}^+(n) : \text{trace}(M) = 1\}$ is a convex and compact base of the cone Sym$^+$(n). It is known [1] that the matrices $v\,v^\top$ with unit vectors $v \in I\!R^n$, $\|v\| = 1$ are the extreme points of the set $\{M \in \text{Sym}^+(n) : \text{trace}(M) = 1\}$ [1]. They have by construction rank 1 and for any unit vector v we find $v\,v^\top v = v \cdot \|v\|^2 = v$ which implies that 1 is the only non-zero eigenvalue. Hence trace($v\,v^\top$)= 1 . Because of this extremal property the matrices $v\,v^\top$ with $\|v\| = 1$ carry the complete information about the base of Loewner ordering cone: convexhull($\{v\,v^\top : v \in I\!R^n,\ \|v\| = 1\}$) is a base for the Loewner ordering cone.

The *penumbra* $P(M)$ of a matrix $M \in$ Sym(n) is the set of matrices N that are smaller than M w.r.t. the Loewner ordering:

$$P_0(M) := \{N \in \text{Sym(n)} : N \leq M\} = M - \text{Sym}^+(n)\,,$$

where we used the customary notation $a + r\,S := \{a + r \cdot s : s \in S\}$ for a point $a \in V$, a scalar r and a subset $S \subset V$.

Using this geometric description the problem of finding the maximum of a set of matrices $\{A_1, \ldots, A_m\}$ amounts to determining the minimal penumbra covering their penumbras $P_0(A_1), \ldots, P_0(A_m)$. Its vertex represents the wanted maximal matrix $\overline{A}$ that dominates all A_i w.r.t the Loewner ordering.

However, the cone itself is too complicated a structure to be handled directly. Instead we associate with each matrix $M \in \text{Sym(n)}$ a *ball* in the subspace $\{A : \text{trace}(A) = 0\}$ of all matrices with zero trace as a *completely descriptive set*. We will assume for the sake of simplicity that $\text{trace}(M) \geq 0$. This ball is constructed in two steps: First, from the statements above we infer that the set $\{M - \text{trace}(M) \cdot \text{convexhull}\{v\, v^\top : v \in I\!R, \|v\| = 1\}\}$ is a base for $P_0(M)$ contained in the subspace $\{A : \text{trace}(A) = 0\}$. We observe that the identity matrix E is perpendicular to the matrices A from this subspace, $\langle A, E\rangle = \sqrt{\text{trace}(A)} = 0$, and hence the orthogonal projection of M onto $\{A : \text{trace}(A) = 0\}$ is given by

$$m := M - \frac{\text{trace}(M)}{n} E\,.$$

Second, the extreme points of the base of $P_0(M)$ are lying on a sphere with center m and radius

$$r := \|M - \text{trace}(M) v\, v^\top - m\| = \text{trace}(M)\sqrt{1 - \frac{1}{n}}\,.$$

Consequently, if the center m and radius r of a sphere in $\{A \in \text{Sym}(n) : \text{trace}(A) = 0\}$ are given the vertex M of the associated penumbra $P_0(M)$ is obtained by

$$M = m + \frac{r}{n} \frac{1}{\sqrt{1 - \frac{1}{n}}}\, E\,.$$

With this information at our disposal, we can reformulate the task of finding a suitable maximal matrix $\overline{A}$ dominating the matrices $\{A_1, \ldots, A_m\}$: The *smallest* sphere enclosing the spheres associated with $\{A_1, \ldots, A_m\}$ determines the matrix $\overline{A}$ that dominates the A_i. It is minimal in the sense, that there is no smaller one w.r.t. the Loewner ordering which has this "covering property" of its penumbra.

This is a non trivial problem of computational geometry and we tackle it by using a sophisticated algorithm implemented by B. Gaertner [6]. Given a set of points in $I\!R^d$ it is capable of finding the smallest ball enclosing these points. Hence for each $i = 1, \ldots, m$ we sample within the set of extreme points $\{A_i - \text{trace}(A_i) v\, v^\top\}$ of the base of $P_0(A_i)$ by expressing v in 3d-spherical coordinates, $v = (\sin\phi\cos\psi, \sin\phi\sin\psi, \cos\phi)$ with $\phi \in [0, 2\pi[, \psi \in [0, \pi[$.

The case $n = 2$ can be visualised by embedding Sym(2) in $I\!R^3$ via $A = (a_{ij})_{i,j=1,2} \longleftrightarrow (a_{11}, a_{22}, a_{12})$ as it is indicated in Figure 1. The penumbras of the matrices $\{A_1, \ldots, A_m\}$ are covered with the minimal penumbral cone whose vertex is the desired maximal matrix $\overline{A}$. For presentational purposes an additional orthogonal transformation has been applied such that the x-y-plane coincides with $\{A \in \text{Sym}(2) : \text{trace}(A) = 0\}$. The minimal element $\underline{A}$ is

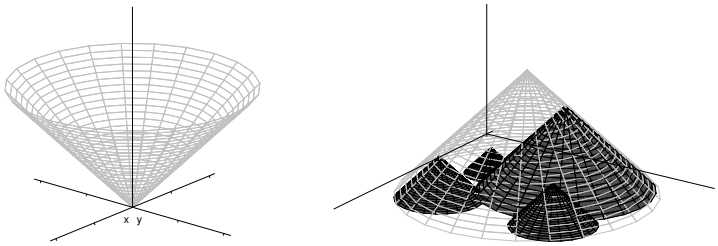

Figure 1. **(a) Left:** Image of the Loewner cone $\mathrm{Sym}^+(2)$. **(b) Right:** Cone covering four penumbras of other matrices. The tip of each cone represents a symmetric 2×2 matrix in $\mathbb{R}^3$. Each of the cones (and hence its generating matrix) is uniquely determined by its circular base. The minimal disc covering the smaller discs belongs to the selected maximal matrix $\overline{A}$

obtained through the formula

$$\underline{A} = \left(\max(A_1^{-1}, \ldots, A_m^{-1})\right)^{-1}$$

inspired by its well-known counterpart for real numbers. The construction of maximal and minimal elements ensures their rotational invariance, their positive semidefiniteness and continuity. These properties are passed on to the above mentioned morphological operations.

3. Experimental Results

In our numerical experiments we use positive definite data. A 128×128 layer of 3-D tensors which has been extracted from a 3-D DT-MRI data set of a human head. For detailed information about the acquisition of this data type the reader is referred to [2] and the literature cited there. The data are represented as ellipsoids via the level sets of the quadratic form $\{x^\top Ax : x \in \mathbb{R}^3\}$ associated with a matrix $A \in \mathrm{Sym}^+(3)$. The color coding of the ellipses reflects the direction of their principle axes.
Due to quantisation effects and measurement imprecisions our DT-MRI data set of a human head contains not only positive definite matrices but also singular matrices and even matrices with negative eigenvalues, though the negative values are of very small absolute value. While such values do not constitute a problem in the dilation process, the erosion, relying on inverses of positive definite matrices, has to be regularised. Instead of the exact inverse A^{-1} of a given matrix A we use $(A + \varepsilon I)^{-1}$ with a small positive ε.

Due to the complexity of the not yet fully optimised procedures the running time to obtain dilation and erosion is about two orders of magnitude longer than in the case of comparable calculations with grey value data.

Figure 2 displays the original head image and the effect of dilation and erosion with a ball-shaped structuring element of radius $\sqrt{5}$. For the sake of brevity we will denote in the sequel this element by BSE($\sqrt{5}$). As it is ex-

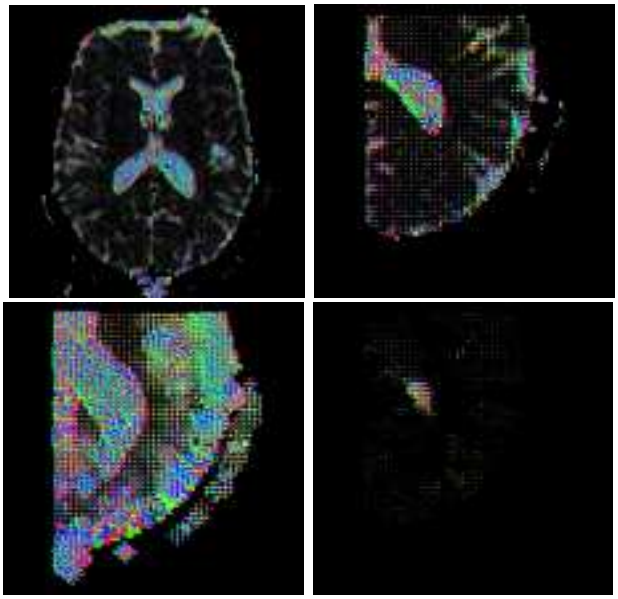

Figure 2. **(a) Top left:** 2-D tensor field extracted from a DT-MRI data set of a human head. **(b) Top right:** enlarged section of left image. **(c) Bottom left:** dilation with BSE($\sqrt{5}$). **(d) Bottom right:** erosion with BSE($\sqrt{5}$).

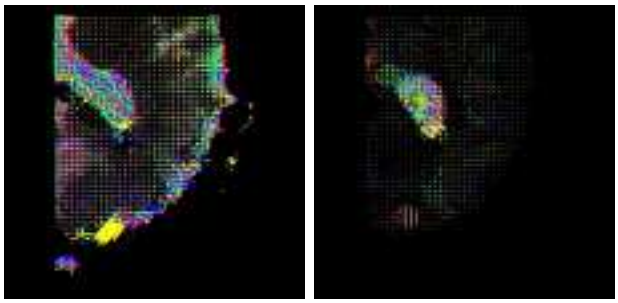

Figure 3. **(a) Left:** closing with BSE($\sqrt{5}$). **(b) Right:** opening with BSE($\sqrt{5}$).

pected from scalar-valued morphology, the shape of details in the dilated and eroded images mirrors the shape of the structuring element. In Figure 3 the results of opening and closing operations are shown. In good analogy to their scalar-valued counterparts, both operations restitute the coarse shape and size of structures. The output of top hat filters can be seen in Figure 4. As in the scalar-valued case, the white top hat is sensitive for small-scale details formed by matrices with large eigenvalues, while the black top hat responds with high values to small-scale details stemming from matrices with small eigenvalues.

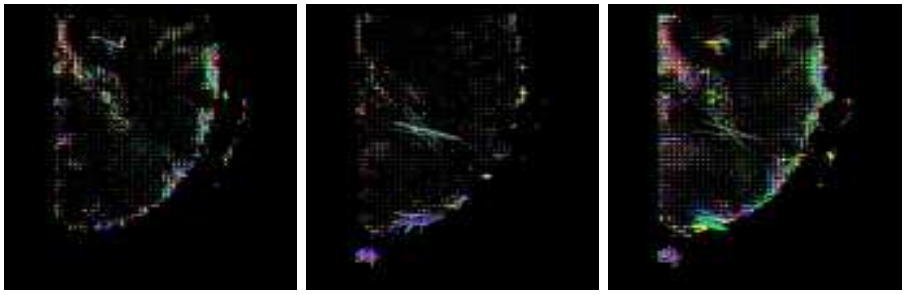

Figure 4. **(a) Left:** white top hat with BSE($\sqrt{5}$). **(b) Middle:** black top hat with BSE($\sqrt{5}$). **(c) Right:** self-dual top hat with BSE($\sqrt{5}$).

Figure 5. **(a) Left:** external gradient with BSE($\sqrt{5}$). **(b) Middle:** internal gradient with BSE($\sqrt{5}$). **(c) Right:** Beucher gradient with BSE($\sqrt{5}$).

Very long ellipses also seen in the yellow spot in Figure 3, are partially artefacts caused by the tool for graphical representation. The self-dual top hat as the sum of white and black top hat results in homogeneously extreme matrices rather evenly distributed in the image.

Figure 5 depicts the effects of internal and external morphological gradients and their sum, the Beucher gradient for our sample matrix field. The action of the Laplacian Δ_{m} and its use for steering a shock filter can be seen in Figure 6: While applying dilation in pixels where the trace of the Laplacian is negative, the shock filter acts as an erosion wherever the trace of the Laplacian is positive. The output is an image where regions with larger and smaller eigenvalues are separated more clearly than in the original image.

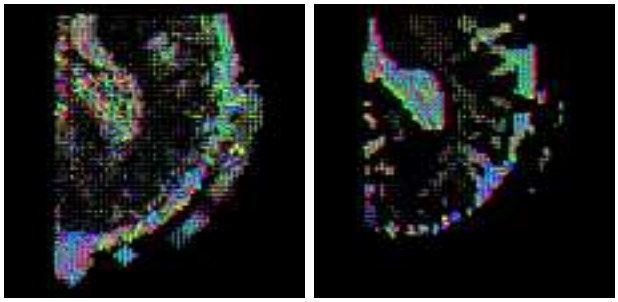

Figure 6. **(a) Left:** morphological Laplacian with BSE($\sqrt{5}$). **(b) Right:** result of shock filtering with BSE($\sqrt{5}$).

4. Conclusion

In this paper we determined suitable maximal and minimal elements $\overline{A}$, $\underline{A}$ in the space of symmetric matrices $\mathrm{Sym}(3)$ with respect to the Loewner ordering. Thus we have been able to transfer fundamental concepts of mathematical morphology to matrix-valued data. The technique developed for this purpose is considerably more general and sustainable than former approaches for the case of 2×2-matrices. The present approach has potential to cope successfully even with 5×5-matrix fields. We obtained appropriate analogs with desirable continuity properties for the notion of maximum and minimum, the corner stones of mathematical morphology. Therefore we succeeded in designing morphological derivatives and shock filters for tensor fields, aside from the standard morphological operations. The practicability of various morphological operations on positive definite matrix-fields is confirmed by several experiments. Future work will focus on faster performance and the development of more sophisticated morphological operators for matrix-valued data.

Acknowledgments

We are grateful to Anna Vilanova i Bartroli (Eindhoven Institute of Technology) and Carola van Pul (Maxima Medical Center, Eindhoven) for providing us with the DT-MRI data set and for discussing data conversion issues. We also thank Prof. Hans Hagen (University of Kaiserslautern) for very helpful discussions.

References

[1] A. Barvinok. *A Course in Convexity*, volume 54 of *Graduate Studies in Mathematics*. American Mathematical Society, Providence, 2002.

[2] P. J. Basser. Inferring microstructural features and the physical state of tissues from diffusion-weighted images. *Nuclear Magnetic Resonance in Biomedicine*, 8:333–344.

Wiley, New York, 1995.

[3] J. M. Borwein and A. S. Lewis. *Convex Analysis and Nonlinear Optimization*. Springer, New York, 1999.

[4] B. Burgeth, M. Welk, C. Feddern, and J. Weickert. Morphological operations on matrix-valued images. In T. Pajdla and J. Matas, editors, *Computer Vision – ECCV 2004*, volume 3024 of *Lecture Notes in Computer Science*, pages 155–167. Springer, Berlin, 2004.

[5] C. Feddern, J. Weickert, B. Burgeth, and M. Welk. Curvature-driven pde methods for matrix-valued images. Technical Report 104, Department of Mathematics, Saarland University, Saarbrücken, Germany, May 2004.

[6] B. Gartner. http://www2.inf.ethz.ch/personal/gaertner/. WebPage last visited: July 2nd, 2004.

[7] J. Goutsias, L. Vincent, and D. S. Bloomberg, editors. *Mathematical Morphology and its Applications to Image and Signal Processing*, volume 18 of *Computational Imaging and Vision*. Kluwer, Dordrecht, 2000.

[8] H. J. A. M. Heijmans. *Morphological Image Operators*. Academic Press, Boston, 1994.

[9] J.-B. Hiriart-Urruty and C. Lemarechal. *Fundamentals of Convex Analysis*. Springer, Heidelberg, 2001.

[10] H. P. Kramer and J. B. Bruckner. Iterations of a non-linear transformation for enhancement of digital images. *Pattern Recognition*, 7:53–58, 1975.

[11] G. Matheron. *Elements pour une theorie des milieux poreux*. Masson, Paris, 1967.

[12] J. Serra. *Echantillonnage et estimation des phenomenes de transition minier*. PhD thesis, University of Nancy, France, 1967.

[13] J. Serra. *Image Analysis and Mathematical Morphology*, volume 1. Academic Press, London, 1982.

[14] J. Serra. *Image Analysis and Mathematical Morphology*, volume 2. Academic Press, London, 1988.

[15] P. Soille. *Morphological Image Analysis*. Springer, Berlin, 1999.

[16] H. Talbot and R. Beare, editors. *Proc. Sixth International Symposium on Mathematical Morphology and its Applications*. Sydney, Australia, April 2002. http://www.cmis.csiro.au/ismm2002/proceedings/.

[17] D. Tschumperle and R. Deriche. Diffusion tensor regularization with contraints preservation. In *Proc. 2001 IEEE Computer Society Conference on Computer Vision and Pattern Recognition*, volume 1, pages 948–953, Kauai, HI, December 2001. IEEE Computer Society Press.

[18] L. J. van Vliet, I. T. Young, and A. L. D. Beckers. A nonlinear Laplace operator as edge detector in noisy images. *Computer Vision, Graphics and Image Processing*, 45(2):167–195, 1989.

[19] J. Weickert and T. Brox. Diffusion and regularization of vector- and matrix-valued images. In M. Z. Nashed and O. Scherzer, editors, *Inverse Problems, Image Analysis, and Medical Imaging*, volume 313 of *Contemporary Mathematics*, pages 251–268. AMS, Providence, 2002.

[20] M. Welk, C. Feddern, B. Burgeth, and J. Weickert. Median filtering of tensor-valued images. In B. Michaelis and G. Krell, editors, *Pattern Recognition*, volume 2781 of *Lecture Notes in Computer Science*, pages 17–24, Berlin, 2003. Springer.